NANO LETTERS

pubs.acs.org/NanoLett

Orientation-Controlled Alignment of Axially Modulated pn Silicon Nanowires

Chi Hwan Lee, Dong Rip Kim, and Xiaolin Zheng*

Department of Mechanical Engineering, Stanford University, Stanford, California 94305, United States

ABSTRACT We demonstrate orientation-controlled alignment of axially modulated pn SiNWs by applying dc electric fields across metal electrodes. The as-aligned pn SiNWs exhibit rectifying behaviors with a 97.7% yield, and about 35% of them exhibit no hysteresis in their current−voltage curves that can be directly used to construct AND/OR logic gates. Moreover, the as-aligned pn SiNWs can be packaged either with polydimethylsiloxane or additional metal layer to protect and even improve the quality of these NW diodes.

KEYWORDS Nanowire alignment, dielectrophoresis, electrophoresis, heterogeneous nanowire, orientation-controlled alignment

To enable wafer-scale fabrication of one-dimensional nanowires (NWs)-based electronic and optical devices, diverse methods have been developed to align NWs, ranging from contact printing method,[1] flow-assisted alignment,[2] Langmuir−Blodgett technique,[3] electric field assisted alignment,[4−17] and blow bubble method,[18] to direct growth of NW devices method.[19] To date, most of these methods have been applied to align axially homogeneous NWs, such as gold, zinc oxide, silicon, and polymer NWs.[4−16] Alignment of axially modulated heterogeneous NWs remains challenging since the orientation of the NWs has to be controlled to correctly express their built-in functionalities.[20,21] Previously, we reported a direct growth of NW devices (DGND) method, for which axially modulated pn SiNWs grow epitaxially between the sidewalls of two heavily doped Si electrodes, and as such alignment and electric contact of NWs are realized simultaneously with the growth step.[19] Nevertheless, the DGND method requires the usage of Si as electrodes for the epitaxial growth of SiNWs. Here, we report a dc electric field-assisted alignment method to align axially modulated pn SiNWs with controlled orientations with a high yield of 97.7% among 177 tests.

The electric field-assisted alignment method[4−17] has been applied to align homogeneous NWs, such as Au NWs,[9] SiNWs[15] and ZnO NWs,[12] normally by the dielectrophoresis (DEP) forces. The DEP forces are exerted on the dielectric NWs through the induced dipoles when the NWs are subjected to a nonuniform electric field.[22,23] However, electric field-assisted alignment of axially modulated NWs, such as pn SiNWs, has not been attempted. Interestingly, the axially modulated pn SiNWs, in comparison to axially homogeneous SiNWs, have not only charge neutral regions, but also charged regions, known as the depletion layer at the pn junction. Therefore, an external nonuniform electric field can interact with the pn SiNWs both through the DEP forces on the induced dipoles and through the electrophoresis (EP) forces on the intrinsic dipoles.[16,22,23] The combination of the DEP and EP forces determines the alignment and orientation of the axially modulated pn SiNWs.

The alignment process of the axially modulated pn SiNWs is conceptually illustrated in Figure 1, where we have assumed that the NWs have comparable lengths to the gap distances between the two electrodes as our experiments so that the NWs bridge the gap after the alignment. When a dc electric field is applied across the two electrodes, the charge neutral regions of the pn SiNWs become polarized which are subjected to the DEP forces (Figure 1a). Since the pn SiNWs are more conductive than the solvent isopropyl alcohol (IPA),[4,23] the pn SiNWs are attracted to the electrode edges where the electric field gradient is the highest (Supporting Information Figure S1).[22,23] The time-averaged DEP force acting on the pn SiNWs is estimated using eq 1[22,23]

$$\overrightarrow{F_{\mathrm{DEP}}} = \frac{\pi r^2 l}{2}\varepsilon_{\mathrm{m}}K(\omega)\cdot\vec{\nabla}|\vec{E}|^2 \qquad (1)$$

where r [m] is the radius of the pn SiNWs, l [m] is the length of the NWs, ε_{m} [F/m] is the permittivity of the suspending medium IPA, $K(\omega)$ is the real part of the Clausius−Mosotti factor, and E [V/m] is the electric field. The maximum DEP force is about 12.5 pN for our pn SiNWs that have an average diameter of 100 nm and length of 12 μm (p- and n- segments are about 6 μm long) and are assumed to lie on a plane 300 nm above the substrate. Previous simulation results[4] have shown that the maximum DEP force acting on silicon carbide (SiC) NWs (diameter, 200 nm; length, 2 μm) lying on a plane 300 nm above the substrate is 1.3 pN, which is in the comparable range of our estimated DEP forces, considering the geometric differences of these two NWs. In addition, the estimated DEP force is much larger than forces caused by the Brownian motions, thermal effects, buoyancy forces, and viscous drag forces,[4,14] so these forces have little

* To whom correspondence should be addressed. E-mail: xlzheng@stanford.edu.
Received for review: 10/15/2010
Published on Web: 11/02/2010

DOI: 10.1021/nl103630c | *Nano Lett.* **2010,** *10,* 5116–5122

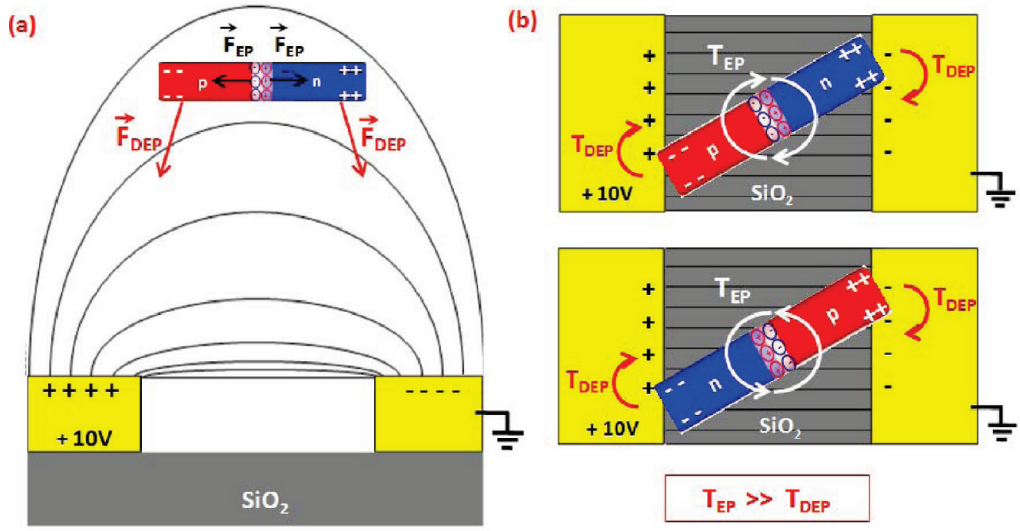

FIGURE 1. Schematics of the orientation-controlled alignment of the axially modulated pn SiNWs with a dc electric field. (a) Side view showing that the pn SiNW is attracted by the DEP forces toward the electrode edges where they have the largest electric field gradient, and the mass center position of the pn SiNWs cannot be changed by the two EP forces exerted on the charges in the depletion zone since they have the same magnitude but opposite direction. (b) Top view showing that the tilted pn SiNWs rotate under the combined effects of T_{DEP} and T_{EP} torques, which can have different directions depending on the orientation of the pn SiNWs with respect to the external electric field direction. Since T_{EP} is larger than T_{DEP}, the orientation of the axially modulated pn SiNWs is mainly determined by the T_{EP} torque.

impact on the movement of NWs near the electrodes and are neglected here.

Other than the DEP forces, the electric field also applies the EP forces on the charged depletion zone of the pn SiNWs, which can be estimated from eq 2

$$\vec{F}_{EP} = qNV\vec{E} \tag{2}$$

where q [C] is the elementary charge, N [number/m^3] is the number density of either acceptors or donors, and V [m^3] is the volume of the depletion region in the p- or n- segment. The calculated EP force on our pn SiNWs is about 31 pN. Although the estimated EP forces are larger than the estimated DEP forces, the EP forces will not change the center location of the pn SiNWs because the two EP forces act on both sides of the pn junction with the same magnitude but opposite directions (Figure 1a). Nevertheless, the EP forces can generate a torque (T_{EP}) to rotate the pn SiNWs when the NWs are not parallel to the direction of the electric field (Figure 1). The T_{EP} torque achieves its maximum value when the pn SiNWs are perpendicular to the electric field, and its magnitude can be estimated using eq 3

$$\vec{T}_{EP} = \vec{F}_{EP}\left(\frac{w}{2}\right) \tag{3}$$

where w [m] is the width of the depletion layer. The calculated maximum T_{EP} is about 0.8 pN·μm. The pn SiNWs also experiences the torque (T_{DEP}) generated by the DEP force when they are not parallel to the direction of the electric field. The T_{DEP} and T_{EP} torques can have different directions depending on the orientation of the pn SiNWs (Figure 1b), so their competition determines the final orientation of the pn SiNWs. Nevertheless, the T_{DEP} is small when the length of NWs is comparable to the gap distance between the two electrodes, since the direction of the DEP force is almost vertical and its horizontal component, responsible for the T_{DEP} torque, is negligible. The maximum T_{DEP} for SiC NWs with similar dimensions, according to previous simulation,[4] is about 1.5×10^{-4} pN·μm, which is around 10^4 times smaller than our calculated T_{EP} (0.8 pN·μm). Therefore, the T_{EP} is the dominant torque to rotate the pn SiNWs, so the pn SiNWs are aligned with the intrinsic dipole opposite to the direction of the applied electric field.

Experimentally, the axially modulated pn SiNWs are aligned by applying a 10 V dc bias across an electrode pair (see Methods). The alignment process of the pn SiNWs was recorded through a high speed camera (Phantom Miro 3) (Supporting Information, Supplementary Movies), which shows that the pn SiNWs are first attracted to the nearby region of the electrode edges due to the DEP forces, then rotate to the corrected orientation when needed under the dominant influence of the T_{EP} torque, and finally are attached to the electrodes. As such, the aligned pn SiNWs are parallel to the external electric field with the p-segment contacting the higher potential side of the electrode pair (Figure 2a, inset). The quality of the alignment can be clearly seen from the SEM image (Figure 2b) where all the NWs are almost parallel to each other. The density of the as-aligned pn SiNWs can be controlled through the NW concentration in the IPA suspension. The current−voltage (I−V) curves of

DOI: 10.1021/nl103630c | *Nano Lett.* **2010,** *10,* 5116–5122

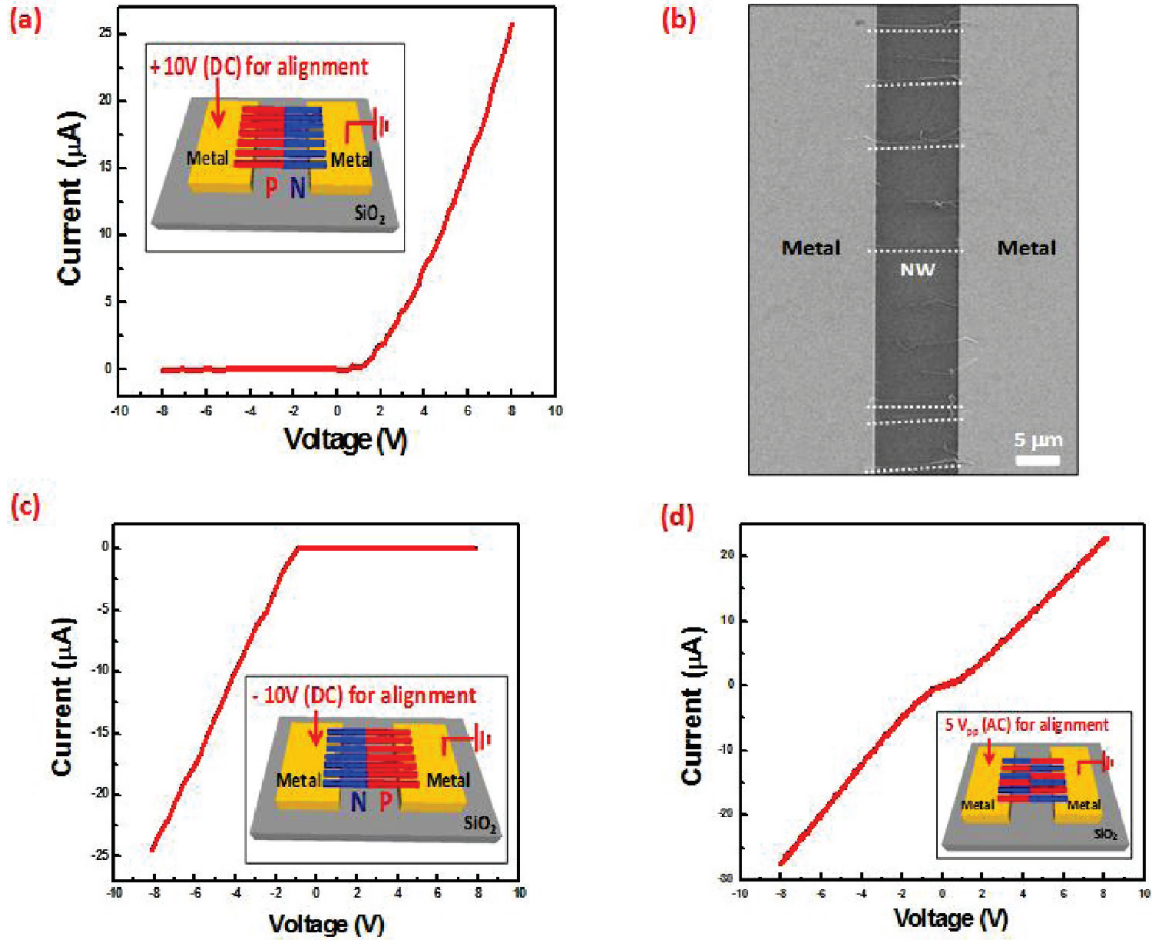

FIGURE 2. Electrical transport of the as-aligned pn SiNWs. (a) $I-V$ curves of the as-aligned pn SiNWs exhibit forward-biased rectifying behavior. The schematic (inset) shows the final orientation of the as-aligned SiNWs when a 10 V dc voltage is applied to the left-hand side electrode. (b) SEM images of the as-aligned pn SiNWs between two electrodes. (c) $I-V$ curves of the as-aligned pn SiNWs show reverse-biased rectifying behavior when a −10 V dc voltage is applied to the left-hand side electrode. (d) $I-V$ curves of the as-aligned pn SiNWs are nonlinear without rectifying behavior when ac voltages (5 V_{pp}, 102 kHz) are applied.

the as-aligned pn SiNWs show good rectifying behaviors (Figure 2a), confirming the orientation-controlled alignment of the pn SiNWs, and their diode quality factors (n) have a normal distribution of 2.12 ± 0.31 summarized over 20 devices. The alignment direction of the pn SiNWs can be reversed by applying a negative potential (−10 V, dc) to the left-hand side electrode such that reversed rectifying behaviors are realized (Figure 2c). The above orientation-controlled alignment of pn SiNWs suggests that T_{EP}, not T_{DEP}, is the dominant torque for rotating NWs, so that the final orientation of pn SiNWs is determined by their intrinsic dipole moments, which needs to be opposite to the direction of the external electrical field to minimize the electric potential energy. To further confirm the dominant role of T_{EP} in alignment, we applied alternating current (ac) sine wave voltages (5 V_{pp}, 102 kHz) to change the direction of T_{EP} periodically so that the pn SiNWs were rotated back and forth. As expected, nonlinear $I-V$ curves (Figure 2d) are observed indicating that the pn SiNWs are aligned with random orientations (Figure 2d, inset). These experimental results demonstrate that the axially modulated pn SiNWs are controllably rotated and aligned by using dc electric fields.

We further deposited platinum (Pt) on top of the pn SiNWs to confirm that the rectifying behavior of the pn SiNW diodes comes from the NWs themselves, not from the asymmetric NW−metal contact.[12] A 200 nm thick of Pt film was deposited on all the pn SiNWs that bridge a metal electrode pair by using a focused ion beam (FIB) (Figure 3a). Before depositing Pt, as shown in Figure 3b, the as-aligned pn SiNWs exhibit rectifying behavior but with hysteresis, indicating that the metal-NW contact resistance is high. Such rectifying $I-V$ curves with hysteresis are observed for about 65% of the as-aligned pn SiNW devices. After depositing Pt, the hysteresis is removed and the current level is also increased significantly (Figure 3b), implying that the NW−metal contact resistance has been reduced effectively. Importantly, the rectifying characteristics of the $I-V$ curves are preserved (Figure 3b), so it confirms that the rectification behavior comes from the pn SiNWs which are aligned with controlled orientations.

DOI: 10.1021/nl103630c | *Nano Lett.* **2010,** *10,* 5116–5122

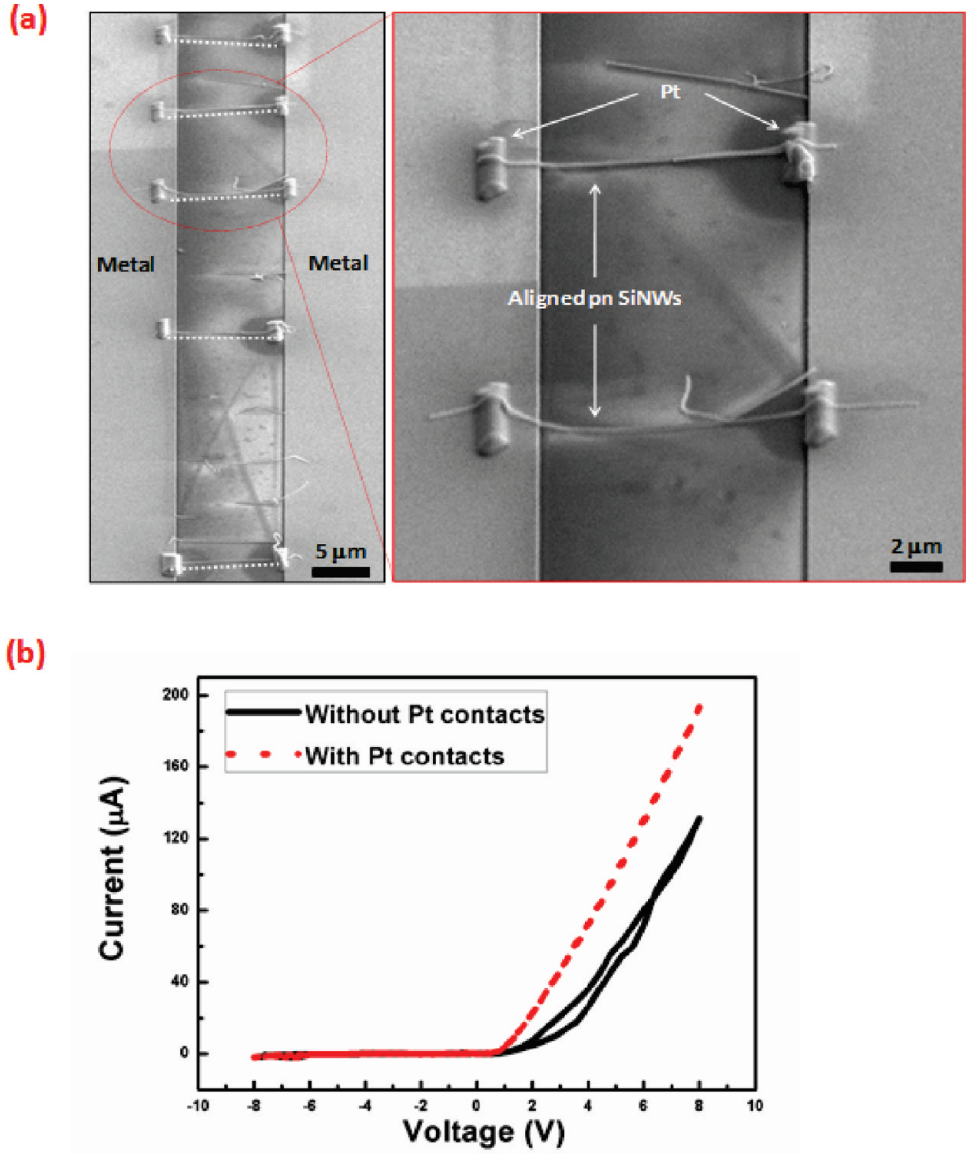

FIGURE 3. Identify the origin of the rectifying behavior of the as-aligned pn SiNWs by adding a top Pt layer. (a) SEM images show that a 200 nm thick Pt layer was deposited on both ends of the as-aligned pn SiNWs by FIB. (b) $I-V$ curves of the as-aligned pn SiNWs with (dotted lines) and without Pt (straight lines). After depositing the Pt layer, the hysteresis is removed and the current level is increased, but the rectifying behavior is retained. So the rectifying behavior comes from the pn SiNWs and not the NW−metal contact.

We have performed 177 alignment tests with different metal electrode gap distances and achieved a 97.7% yield of the forward-biased diodes, and the rest 2.3% devices (4 out of 177) have nonlinear $I-V$ curves without rectifying properties (Supporting Information, Table S1). The nonlinear $I-V$ curves could come from very poor metal−NW contact quality or disorientated pn SiNWs, which can occur due to the physical interference from the neighboring NWs.[14] Nevertheless, no reverse-rectifying behaviors were observed for the 177 tests. The statistical data strongly supports that the dc electric field-assisted alignment of the axially modulated pn SiNWs provides excellent control of orientation with high yield.

As discussed above, roughly 35% of the as-aligned pn SiNWs have excellent rectifying $I-V$ curves without hysteresis. To further test the quality of these as-aligned pn SiNW diodes, we applied them directly to construct the OR and AND diode logic gates. A number of pn SiNWs were aligned across two different pairs of electrodes to construct two diodes and an external resistor of 25 MΩ was connected for the test. Figure 4 illustrates the schematics (left) and characteristics (right) of both logic gates. For both gates, all the voltage inputs (V_{in1} and V_{in2}) when on high are 5 V provided by an external power supply. For the OR logic gate, when either of the input voltages is high (5 V), the output voltage V_{out} is high (Figure 4a, right). Likewise, for the AND logic gate, only when both inputs V_{in1} and V_{in2} are high (5 V), the output voltage V_{out} is high (Figure 4b, right). The observed rectifying characteristics of OR and AND logic gates

DOI: 10.1021/nl103630c | *Nano Lett.* **2010,** *10,* 5116–5122

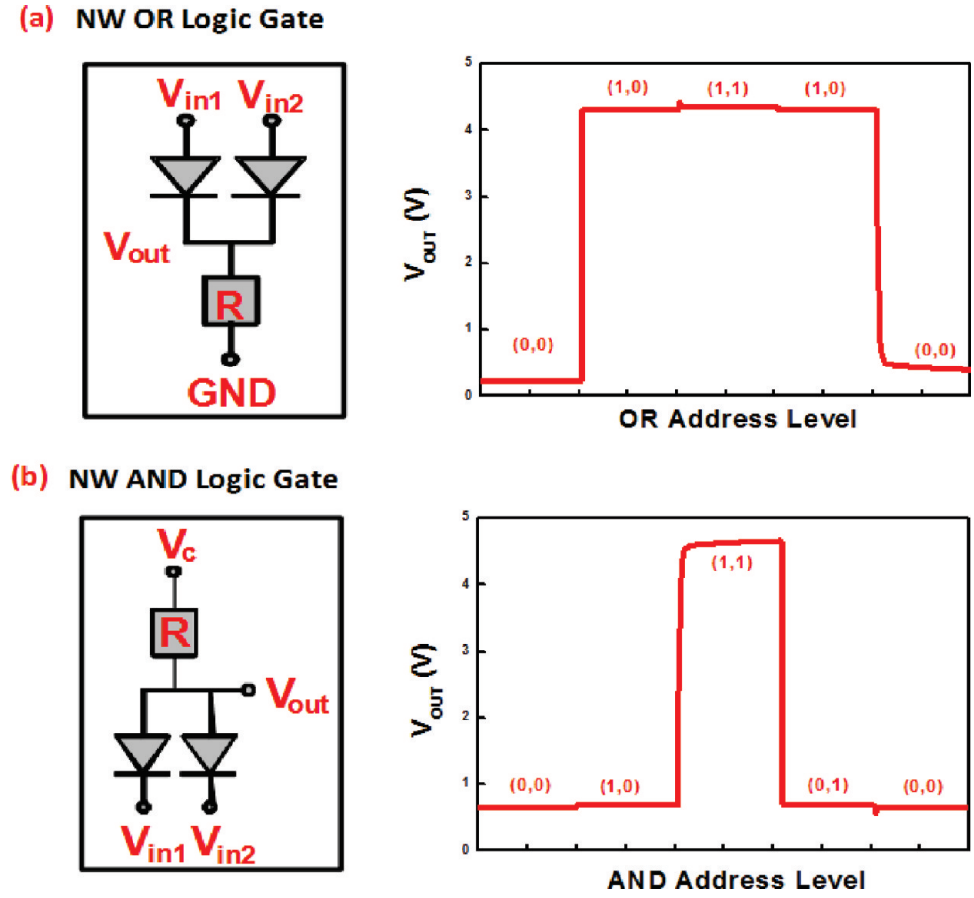

FIGURE 4. OR and AND diode logic gates constructed with the as-aligned pn SiNWs. (a) Schematics of the pn SiNWs OR logic gate (left). The output voltage V_{out} is 1 when either V_{in1} and V_{in2} is 1, or both are 1 (right). (b) Schematics of the pn SiNWs AND logic gate (left), where V_c is the supply voltage. The output voltage V_{out} is 1 only when both V_{in1} and V_{in2} are 1 (right). For both the OR and AND gates measurements, logic 0 input is 0 V; logic 1 input is 5 V; and a 25 MΩ external resistor was used to balance the diode resistance.

further support the good quality of the orientation-controlled alignment of the pn SiNWs and the NW−metal contact.

Even though the as-aligned pn SiNWs with good rectifying properties can be readily used as diodes and components of logic gates, these NW devices need to be packed to immobilize NWs and protect or even improve the quality of the NW−metal contact. Packaging these NWs with metal deposition by FIB as shown early is not practical for wafer-scale fabrication due to the time-consuming serial deposition of FIB. Here, we propose two methods to pack the as-aligned NW devices depending on the original quality of the diodes. The first method is used when the as-aligned pn SiNWs have good rectifying characteristics without hysteresis, and the NW devices are simply encapsulated by polydimethylsiloxane (PDMS). The liquid PDMS is poured directly onto the as-aligned pn SiNW devices and cured overnight at room temperature. The liquid PDMS, due to its low viscosity and low surface energy, penetrates into the gaps between NWs and metals, and fully encapsulates the NW devices,[24] as shown in the inset of Figure 5a, where two tungsten wires are embedded inside PDMS for electrical measurements. As shown in Figure 5, the PDMS encapsulation step has negligible effect on the $I-V$ curves of the original as-aligned pn SiNW devices, and more importantly, the rectifying $I-V$ curves are preserved even after one month of PDMS encapsulation, suggesting that PDMS effectively protects the devices from environmental damage.

The second packaging method essentially adds another metal contact layer (Ti 5 nm/Pd 150 nm) on top of the pn SiNWs by using photolithography (Figure 5b). The additional metal layer not only fixes the locations of the NWs, but also improves the NW−metal contact quality. For the contact improvement, the surface native oxide of the pn SiNWs is removed with a buffered oxide etchant (BOE, 20:1) right before the deposition of the top metal layer. As shown in Figure 5b, after adding the top metal layer, the hysteresis of the original $I-V$ curves is removed. This method is suitable for packing all the pn SiNWs at the wafer scale, in particular for those as-aligned pn SiNWs devices with hysteretic $I-V$ curves. These two packaging methods provide effective means to bridge orientation-controlled alignment of the axially modulated pn SiNWs with functional and robust NW devices.

In summary, we have demonstrated orientation-controlled alignment of the axially dopant-modulated pn SiNWs across metal electrode pairs with dc electric fields. The pn

DOI: 10.1021/nl103630c | *Nano Lett.* **2010,** *10,* 5116–5122

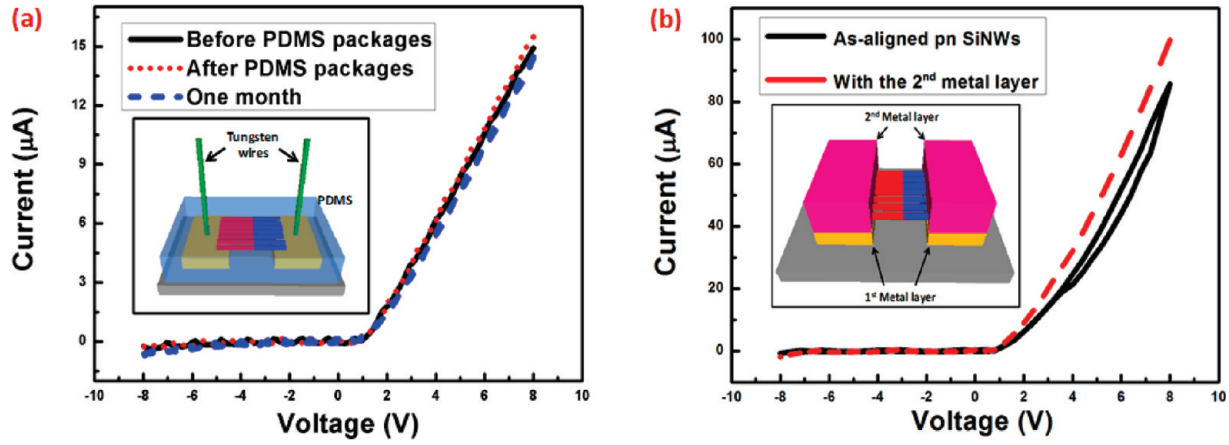

FIGURE 5. Two packaging methods for the as-aligned pn SiNWs to preserve the location of the NWs and protect or improve the quality of the NW−metal contacts. (a) The inset schematic shows that the as-aligned pn SiNWs are fully encapsulated by PDMS and the two tungsten wires embedded inside PDMS are for electrical measurements. The rectifying $I-V$ curves are not affected by the encapsulation process and are preserved after one month. (b) The inset shows that additional metal contact layer (Ti 5 nm/Pd 150 nm) is added on top of the as-aligned pn SiNWs by using photolithography. After adding the top metal contact layer, the hysteresis in the original $I-V$ curve is completely removed and the current level through the NWs is increased as well.

SiNWs suspended in IPA are attracted to the electrode edges by the DEP forces and rotated by the T_{EP} torques, and their intrinsic dipole moments are aligned at the opposite direction of the external electric field finally. About 97.7 % of the as-aligned pn SiNWs have rectifying $I-V$ behaviors and 35 % of them have no hysteresis with an average diode quality factor of 2.12. These good quality diodes can be directly used to construct the OR and AND diode logic gates with high performance. Furthermore, we have confirmed that the origin of the rectifying behaviors come from the as-aligned pn SiNWs, not from the NW−metal contact. Finally, we demonstrated two effective packaging methods, that is, PDMS encapsulation and addition of a top metal layer, to immobilize the as-aligned NWs and to protect or even improve the quality of the NW−metal contact. We believe that the high-yield orientation-controlled, dc electric field-assisted alignment of the axially modulated pn SiNWs, together with the two packaging methods, can open up new opportunities for developing heterogeneous NW-based devices at the wafer scale.

Methods. ***Synthesis of the Axially Modulated pn SiNWs.*** The NWs were grown by the vapor−liquid−solid (VLS) growth mechanism using gold particles (100 nm diameter) as the catalyst.[25] During the growth period, the precursor gases are changed to axially modulate the chemical composition of the SiNWs. For the pn SiNWs, the feeding ratio of silane to dopant (boron) for the p-segment is 4000:1 and the growth conditions are 650 °C, 5 Torr, 712 sccm of H_2, 30 sccm of SiH_4, 30 sccm of HCl, and 37.5 sccm of 10 000:1 H_2 diluted B_2H_6. For the n-segment, the feeding ratio of silane to dopant (phosphorus) is 1500:1 and the growth conditions are 650 °C, 5 Torr, 730 sccm of H_2, 30 sccm of SiH_4, 30 sccm of HCl, and 20 sccm of 1000:1 H_2 diluted PH_3. The length of the pn SiNWs is controlled by the growth time and targeted for 6 μm for both the p- and n-segments.

dc Electric Field-Assisted Alignment of the Axially Modulated pn SiNWs. After growth, the axially modulated pn SiNWs are sonicated off from their growth substrate in IPA to form a suspension. A drop of the suspension is deposited on top of electrode pairs (5 mm wide × 5 mm long, and 150 nm in height) predefined by photolithography. The gap between the electrode pairs varies from 9 to 13 μm so that the gap distances are comparable to the lengths of NWs.

Electrical Measurements and Image Recording. The $I-V$ curves were recorded using a semiconductor analyzer (Keithley, model SCS 4200) in a probe station (Signatone). The diode quality factor (n) was extracted from the dark $I-V$ curves using the ideal diode equation $\ln(I) = (q/nkT)V + \ln(I_0)$ where q is the elementary charge, k is the Boltzmann constant, T is the temperature, and I_0 is the saturation current. The alignment process of the pn SiNWs was recorded in a microscope system (Olympus, U-CMAD3) with a high speed camera (Phantom).

Acknowledgment. X.L.Z. sincerely thanks NSF (Award Number 0826003) and Center for Integrated Systems of Stanford University for support of this work. D.R.K acknowledges support from the Link Foundation Energy Fellowship. The authors also thank to Professor Juan G. Santiago and Alexandre Persat at Stanford University for their help with recording the alignment process of the axially modulated pn SiNWs.

Supporting Information Available. Additional figure and table and videos. This material is available free of charge via the Internet at http://pubs.acs.org.

REFERENCES AND NOTES

(1) Fan, Z. Y.; Ho, J. C.; Jacobson, Z. A.; Yerushalmi, R.; Alley, R. L.; Razavi, H.; Javey, A. *Nano Lett.* **2008**, *8* (1), 20–25.
(2) Huang, Y.; Duan, X. F.; Wei, Q. Q.; Lieber, C. M. *Science* **2001**, *291* (5504), 630–633.

(3) Dongmok, W.; Song, J.; Yue, W.; Lieber, C. M. *Nano Lett.* **2003**, *3* (9), 1255–1259.
(4) Liu, Y. L.; Chung, J. H.; Liu, W. K.; Ruoff, R. S. *J. Phys. Chem. B* **2006**, *110* (29), 14098–14106.
(5) Duchamp, M.; Lee, K.; Dwir, B.; Seo, J. W.; Kapon, E.; Forro, L.; Magrez, A. *Acs Nano* **2010**, *4* (1), 279–284.
(6) Yaping, D.; Yanyan, C.; Mallouk, T. E.; Johnson, A. T.; Evoy, S. *Sens. Actuators, B* **2007**, 55–59.
(7) Evoy, S.; DiLello, N.; Deshpande, V.; Narayanan, A.; Liu, H.; Riegelman, M.; Martin, B. R.; Hailer, B.; Bradley, J. C.; Weiss, W.; Mayer, T. S.; Gogotsi, Y.; Bau, H. H.; Mallouk, T. E.; Raman, S. *Microelectron. Eng.* **2004**, *75* (1), 31–42.
(8) Lifeng, D.; Bush, J.; Chirayos, V.; Solanki, R.; Jun, J.; Ono, Y.; conley, J. F.; Ulrich, B. D. *Nano Lett.* **2005**, *5* (10), 2112–2115.
(9) Boote, J. J.; Evans, S. D. *Nanotechnology* **2005**, *16* (9), 1500–1505.
(10) Kim, T. H.; Lee, S. Y.; Cho, N. K.; Seong, H. K.; Choi, H. J.; Jung, S. W.; Lee, S. K. *Nanotechnology* **2006**, *17* (14), 3394–3399.
(11) Smith, P. A.; Nordquist, C. D.; Jackson, T. N.; Mayer, T. S.; Martin, B. R.; Mbindyo, J.; Mallouk, T. E. *Appl. Phys. Lett.* **2000**, *77* (9), 1399–1401.
(12) Chang Shi, L.; Jin, L.; Puxian, G.; Liyuan, Z.; Davidovic, D.; Tummala, R.; Wang, Z. L. *Nano Lett.* **2006**, *6* (2), 263–266.
(13) Raychaudhuri, S.; Dayeh, S. A.; Wang, D. L.; Yu, E. T. *Nano Lett.* **2009**, *9* (6), 2260–2266.
(14) Freer, E. M.; Grachev, O.; Stumbo, D. P. *Nat. Nanotechnol.* **2010**, S25–S30.
(15) Englander, O.; Christensen, D.; Kim, J.; Lin, L. W.; Morris, S. J. S. *Nano Lett.* **2005**, *5* (4), 705–708.
(16) Fan, D. L.; Cammarata, R. C.; Chien, C. L. *Appl. Phys. Lett.* **2008**, *92* (9), 093115.
(17) Donglei, F.; Zhizhong, Y.; Cheong, R.; Zhu, F. Q.; Cammarata, R. C.; Chien, C. L.; Levchenko, A. *Nat. Nanotechnol.* **1999**, *5* (7), 545–551.
(18) Yu, G. H.; Cao, A. Y.; Lieber, C. M. *Nat. Nanotechnol.* **2007**, *2* (6), 372–377.
(19) Kim, D. R.; Lee, C. H.; Zheng, X. L. *Nano Lett.* **2010**, *10* (3), 1050–1054.
(20) Yang, C.; Barrelet, C. J.; Capasso, F.; Lieber, C. M. *Nano Lett.* **2006**, *6* (12), 2929–2934.
(21) Kempa, T. J.; Tian, B. Z.; Kim, D. R.; Hu, J. S.; Zheng, X. L.; Lieber, C. M. *Nano Lett.* **2008**, *8* (10), 3456–3460.
(22) Pohl, H. A.; Crane, J. S. *J. Theor. Biol.* **1972**, *37* (1), 1–13.
(23) Pohl, H. A. *Dielectrophoresis*; Cambridge University Press: Cambridge, 1978.
(24) Sun, Y. G.; Choi, W. M.; Jiang, H. Q.; Huang, Y. G. Y.; Rogers, J. A. *Nat. Nanotechnol.* **2006**, *1* (3), 201–207.
(25) Wagner, R. S.; Ellis, W. C. *Appl. Phys. Lett.* **1964**, *4* (5), 89.

DOI: 10.1021/nl103630c | *Nano Lett.* **2010,** *10,* 5116–5122